How to cite: *Angew. Chem. Int. Ed.* **2024**, *63*, e202313067
doi.org/10.1002/anie.202313067

Topochemistry

# Disproportionation of $Co^{2+}$ in the Topochemically Reduced Oxide $LaSrCoRuO_5$

*Zhilin Liang, Maria Batuk, Fabio Orlandi, Pascal Manuel, Joke Hadermann, and Michael A. Hayward**

**Abstract:** Complex transition-metal oxides exhibit a wide variety of chemical and physical properties which are a strong function the local electronic states of the transition-metal centres, as determined by a combination of metal oxidation state and local coordination environment. Topochemical reduction of the double perovskite oxide, $LaSrCoRuO_6$, using Zr, yields $LaSrCoRuO_5$. This reduced phase contains an ordered array of apex-linked square-based pyramidal $Ru^{3+}O_5$, square-planar $Co^{1+}O_4$ and octahedral $Co^{3+}O_6$ units, consistent with the coordination-geometry driven disproportionation of $Co^{2+}$. Coordination-geometry driven disproportionation of $d^7$ transition-metal cations (e.g. $Rh^{2+}$, $Pd^{3+}$, $Pt^{3+}$) is common in complex oxides containing 4d and 5d metals. However, the weak ligand field experienced by a 3d transition-metal such as cobalt leads to the expectation that $d^{7+}$ $Co^{2+}$ should be stable to disproportionation in oxide environments, so the presence of $Co^{1+}O_4$ and $Co^{3+}O_6$ units in $LaSrCoRuO_5$ is surprising. Low-temperature measurements indicate $LaSrCoRuO_5$ adopts a ferromagnetically ordered state below 120 K due to couplings between $S = {}^1/_2$ $Ru^{3+}$ and $S = 1$ $Co^{1+}$.

Complex metal oxides have been the subject of extensive study due to the wide variety properties they exhibit. These range from electronic and magnetic behaviors such as ferroelectricity, superconductivity and magnetoresistance to an extensive array of catalytic and electrochemical phenomena. As the chemical and physical behaviors exhibited by metal oxides tend to depend strongly on the electric configurations of the metal cations they contain (defined by a combination of oxidation states and coordination environments), there has been an enduring interest in establishing composition-structure-property relations in extended oxide systems to explore these features. These studies have revealed that a number of elements exhibit 'disfavored' oxidation states in oxide environments, i.e. oxidation states that appear to be thermodynamically accessible (sufficient lattice energy to overcome the required ionization energy) but are unstable with respect to disproportionation, when the metal is located in an extended oxide framework.

The instability of some of these disfavored states, such as the disproportionation of $Pb^{3+}$ and $Bi^{4+}$ in $Pb_2O_3$ and $BiO_2$ respectively,[1–2] can be accounted for by universal chemical concepts—in this instance the global instability of $ns^1$ electron configurations in main group metals leads to $Pb_2O_3$ and $BiO_2$ being better described as $Pb^{II}Pb^{IV}O_3$ and $Bi^{III}Bi^{V}O_4$ respectively.

However, similar disproportionations are observed in transition-metal systems, where the instability of the metal oxidation state cannot be easily attributed to a global instability of a particular electron count but appears to arise from the favorability of particular combinations of d-electron count and local coordination environment. For example, AgO is better described as $Ag^{I}Ag^{III}O_2$,[3] with the disproportionation of $Ag^{II}$ attributed to the favorability of locating $d^{10}$ $Ag^{I}$ in a linear coordination and $d^8$ $Ag^{III}$ in square-planar coordination sites within the oxide framework. Likewise, analogous disproportionations of $d^7$ cations, such as $Pd^{III}$ or $Pt^{III}$ are observed, driven by the favorability of locating $d^6$ $Pd^{IV}/Pt^{IV}$ cations in octahedral environments and $d^8$ $Pd^{II}/Pt^{II}$ cations in square-planar coordinations, in phases such as $K_2Pd^{II}{}_3Pd^{IV}O_6$ and $CdPt^{II}Pt^{IV}{}_2O_6$.[4–5]

Recently we observed the disproportionation of $d^7$ $Rh^{II}$ during the topochemical reduction of the Ruddlesden-Popper $LaSrM_{0.5}Rh_{0.5}O_4$ (M=Co, Ni) and perovskite $LaM_{0.5}Rh_{0.5}O_3$ oxides, with the reduced phases ($LaSrM_{0.5}Rh_{0.5}O_{3.25}$ and $LaM_{0.5}Rh_{0.5}O_{2.25}$ respectively) hosting $d^8$ $Rh^{I}$ in square-planar coordination sites, and $d^6$ $Rh^{III}$ in 5-coordinate, square-based pyramidal sites.[6–7] Here we describe the first observation of the disproportionation of $d^7$ $Co^{II}$ in an extended oxide, which occurs during the topochemical reduction of the double perovskite oxide $LaSrCoRuO_6$ to $LaSrCoRuO_5$.

Previous work revealed that rapidly quenching the double perovskite oxide $LaSrNiRuO_6$ through a *R*-3 to $P2_1/n$ phase transition ($T \approx 400\,^{\circ}C$)[8] increased the reactivity of this oxide phase with $CaH_2$, allowing the preparation of the

[*] Z. Liang, M. A. Hayward
Department of Chemistry, Inorganic Chemistry Laboratory, University of Oxford
South Parks Road, Oxford OX1 3QR (UK)
E-mail: michael.hayward@chem.ox.ac.uk
M. Batuk, J. Hadermann
EMAT, University of Antwerp
Groenenborgerlaan 171, 2020 Antwerp (Belgium)
F. Orlandi, P. Manuel
ISIS Neutron and Muon Source, Rutherford Appleton Laboratory
Chilton, Oxon OX11 0QX (UK)

infinite layer phase, $LaSrNiRuO_4$, by topochemical anion deintercalation.[9–10] The corresponding cobalt phase, $LaSrCoRuO_6$,[11–12] exhibits an analogous phase transition at $T \approx 450\,^{\circ}C$. Rapidly quenching $LaSrCoRuO_6$ through its $R$-3 to $P2_1/n$ phase transition also enhances its reactivity enabling the preparation of the infinite layer phase $LaSrCoRuO_4$ via reaction with binary metal hydrides, as will be described in detail elsewhere. However, in contrast to the $LaSrNiRuO_{6-x}$ system, quenched samples of $LaSrCoRuO_6$ can be reduced to a phase of intermediate oxygen content (shown to be $LaSrCoRuO_5$ by oxidative thermogravimetric analysis) by reaction with a Zr getter at 450 °C.

Synchrotron X-ray powder diffraction (SXRD) data collected from $LaSrCoRuO_5$ could be indexed using a body-centered monoclinic unit cell ($a = 5.40$ Å, $b = 5.41$ Å, $c = 8.16$ Å, $\gamma = 90.5$ °) consistent with the retention of the perovskite framework from the $LaSrCoRuO_6$ parent phase. However, close inspection revealed a series of weak additional reflections in the SXRD data that could not be indexed by this cell. Electron diffraction (ED) data collected from $LaSrCoRuO_5$, shown in Figure 1, are consistent with a 2×2×1 cell expansion compared to the $LaSrCoRuO_6$ parent phase ($2\sqrt{2}\times2\sqrt{2}\times2$ compared to a simple $ABO_3$ perovskite unit cell).[13–14] This expanded cell accounts for all the additional weak peaks observed in the SXRD data and can also index neutron powder diffraction (NPD) data collected at room temperature from $LaSrCoRuO_5$.

Considering the $A_2BB'O_5$ composition and the $2\sqrt{2}\times2\sqrt{2}\times2$ cell expansion of the phase, a number of anion-vacancy ordered and B-site cation ordered perovskite structural models were considered for $LaSrCoRuO_5$. It was observed that a good fit to the SXRD and NPD data could be achieved using a model based on the anion-vacancy ordered structure of $LaNi_{0.9}Co_{0.1}O_{2.5}$ which consists of a network of apex-linked 6-coordinate octahedral, 5-coordinate square-based pyramidal and 4-coordinate square planar $BO_x$ units.[15] The model was modified to take account of the rock salt ordering of the Co and Ru cations, so that the Ru centers were exclusively located within 5-coordinate sites, while the Co centers occupied both 6- and 4-coordinate sites within a monoclinic unit cell ($a = 10.8128(2)$ Å, $b = 10.8231(2)$ Å, $c = 8.1626(1)$ Å, $\gamma = 90.55(1)$ °) with $P112_1$ space group symmetry, as shown in Figure 2. The model was refined against the NPD data to achieve a good fit (wRp = 6.33 %) as shown in Figure 1 and described in detail in the Supporting Information.[16]

The crystal structure of $LaSrCoRuO_5$ shown in Figure 2 reveals that the cobalt cations occupy two distinct sites within the oxide framework. A 4-coordinate planar site and a 6-coordniate octahedral site. The location of the cobalt

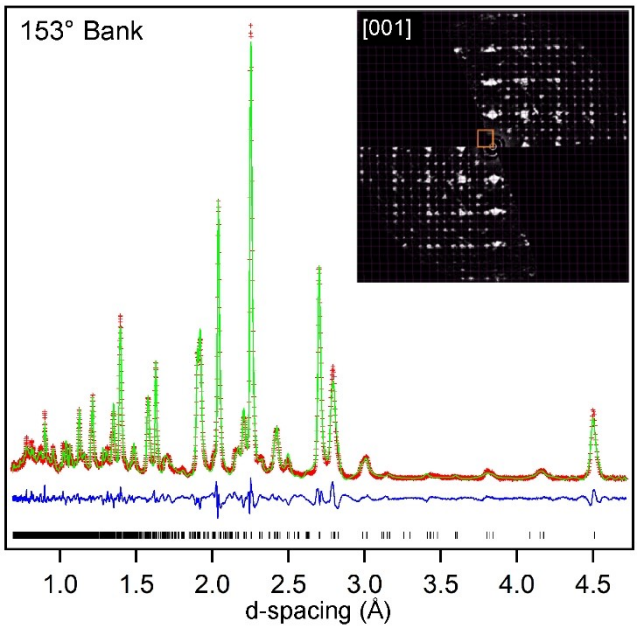


***Figure 1.*** Observed, calculated and difference plots from structural refinement of $LaSrCoRuO_5$ against NPD data. Inset shows ED pattern demonstrating $2\sqrt{2}\times2\sqrt{2}\times2$ cell expansion.

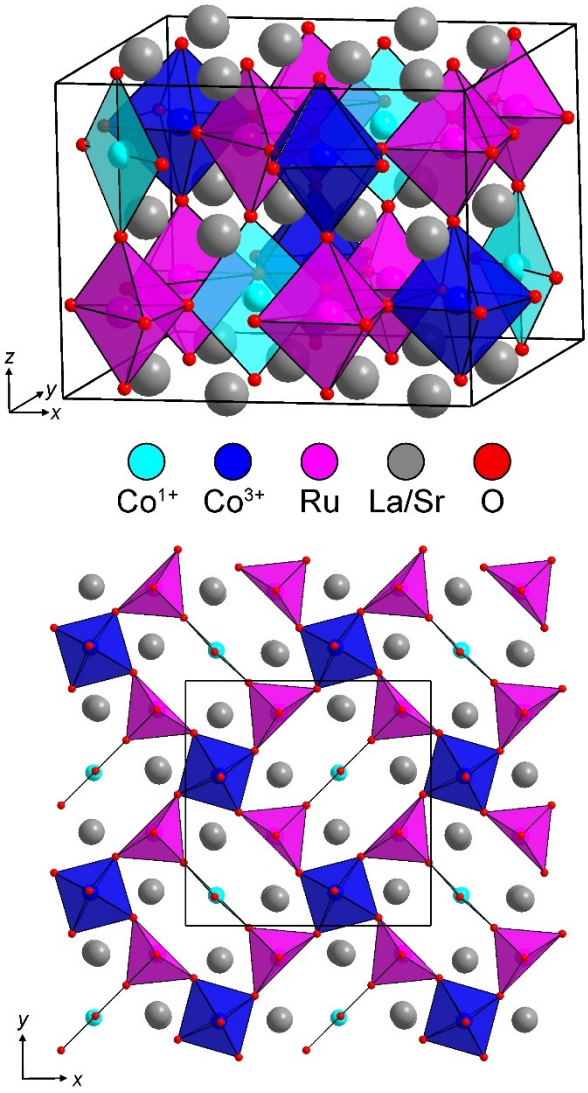


***Figure 2.*** Crystal structure of $LaSrCoRuO_5$ (top) and a projection of the transition metal coordination polyhedra at $z \approx 0.75$ (bottom).

cations in two distinct sites is reminiscent of the local-coordination-driven disproportionation of transition metals with $d^7$ electron counts observed for $Pd^{3+}$ and $Pt^{3+}$ and more recently $Rh^{2+}$, and suggests the disproportionation of $Co^{2+}$ into $Co^{1+}$ (square-planar) and $Co^{3+}$ (octahedral). Analysis of the local coordination environments of the cobalt centers is hampered by the lack of reported $Co^{1+}O_4$ units for comparison. However, the observed bond lengths of the $CoO_4$ units in $LaSrCoRuO_5$ (Co–O = 2.032(11) Å×2; 2.119(9) Å×2) are significantly longer than those in the $Co^{2+}O_4$ units reported in $Sr_3Co_2O_4Cl_2$ (Co–O = 2.007(1) Å×4)[17] or $Sr_2CoO_2Cu_2S_2$ (Co–O = 1.995(1) Å×4)[18] consistent with assignment of $Co^{1+}O_4$ for the units present in $LaSrCoRuO_5$. Bond valance sums (BVS)[19] calculated using parameters for $Co^{2+}$ yield values of $LaSrCoRuO_5$:Co + 1.42, $Sr_3Co_2O_4Cl_2$:Co + 1.70 and $Sr_2CoO_2Cu_2S_2$:Co + 1.76. The $CoO_6$ units in $LaSrCoRuO_5$ have a rather irregular shape but exhibit an average bond length of < Co–O = 2.004 Å > (BVS = Co + 2.69) compared to < Co–O = 2.033 Å > (BVS = Co + 2.38) the $Co^{II}O_6$ units in the $LaSrCoRuO_6$ parent phase.[12] Thus, it can be seen that the BVS values of the square-planar (BVS = Co + 1.42) and octahedral sites (BVS = Co + 2.69) in $LaSrCoRuO_5$ differ by 1.27 units. This difference is significantly larger than the difference between the octahedral and tetrahedral sites in the $Co^{2+}$ brownmillerite phase $La_2Co_2O_5$ ($CoO_6$ BVS = Co + 2.23; $CoO_4$ BVS = Co + 2.07, Δ = 0.16)[20] or the difference between octahedral and square-planar sites in the $Ni^{2+}$ phase $La_2Ni_2O_5$ ($NiO_6$ BVS = 2.08; $NiO_4$ BVS = 2.11, Δ = 0.03)[21] and provides strong support for the disproportionation of $Co^{2+}$ in $LaSrCoRuO_5$.

In an attempt to further confirm the disproportionation of $Co^{2+}$, cobalt EELS data collected from $LaSrCoRuO_5$. These data show a single set of Co $L_2$ and $L_3$ peaks (Figure S14 in the Supporting Information) and thus represent the superposition of signals from both the square-planar and octahedral cobalt sites. In the absence of a $Co^{1+}$ oxide standard we are unable to know if a $Co^{1+}/Co^{3+}$ oxidation state combination would be expected to lead to a resolvable splitting of the $L_2$ and $L_3$ peaks. It should be noted that splitting of $Co^{2+}/Co^{3+}$ signals is not resolvable for $Co_3O_4$.[22] The $L_3/L_2$ intensity ratio (4.83) and $L_3$-$L_2$ energy difference (15.06 eV) from the data are broadly consistent with $Co^{2+}$.

Magnetization data collected from $LaSrCoRuO_5$ indicate that, in common with many other topochemically reduced phases containing cobalt, samples of $LaSrCoRuO_5$ contain small quantities of ferromagnetic, elemental cobalt not detectable by diffraction. The magnetization of $LaSrCoRuO_5$ was therefore measured using the 'ferromagnetic subtraction' method described in the Supporting Information. A plot of the magnetic susceptibility of $LaSrCoRuO_5$ against temperature (Figure 3a) can be fit by the Curie–Weiss law in the range 140 < T/K < 300. However, the extracted Curie constant (C = 3.76 $cm^3 K mol^{-1}$; θ = + 82.7 K) is much larger than can be accounted for by a combination of $Co^{1+}$, $Co^{3+}$ and $Ru^{3+}$ cations (even with the cobalt centers in high-spin states), suggesting strong magnetic interactions are present between the metal centers in this temperature range.

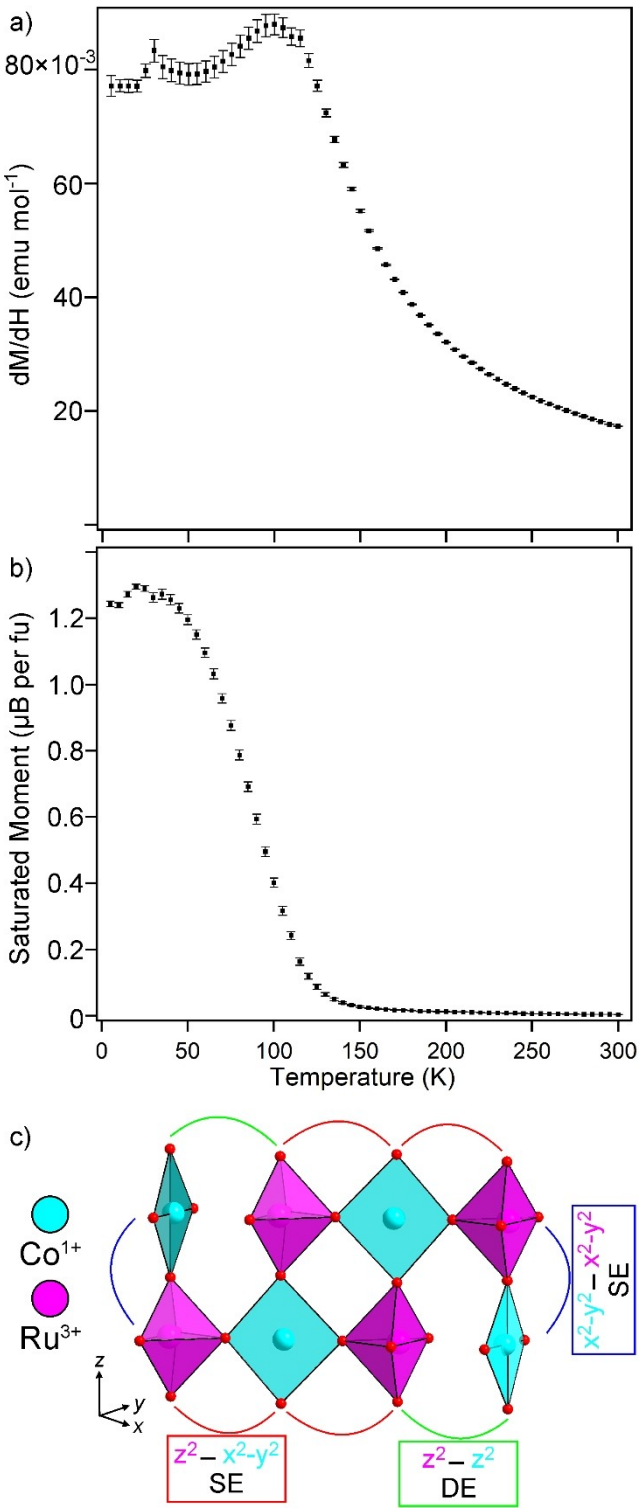


***Figure 3.*** a) Paramagnetic susceptibility and b) saturated ferromagnetic moment of $LaSrCoRuO_5$ measured via the 'ferrosubtraction' method and plotted as a function of temperature, c) The direct exchange and super exchange pathways in $LaSrCoRuO_5$.

On cooling below 120 K there is a large increase in the saturated ferromagnetic moment of the samples (Figure 3b), increasing from 0.03 μB per fu at 150 K (a value that is attributed to the presence of an elemental Co impurity) to ≈1.25 μB per fu at 2 K, indicative of a ferromagnetic state, however NPD data collected at 5 K show no additional features indicative of magnetic order, as described in the Supporting Information.

The bond lengths of the square-planar and octahedral cobalt sites in $LaSrCoRuO_5$ are consistent with a high spin, S = 1 $Co^{1+}$ center, and a low spin, S = 0 $Co^{3+}$ respectively. Thus, the most significant magnetic couplings in the system will be between the square-planar $Co^{1+}$ centers, which have a $(d_{xz/yz})^4(d_{xy})^2(d_{z2})^1(d_{x2-y2})^1$ electronic configuration, and the $Ru^{3+}$ centers located in square-based pyramidal sites which have a $(d_{xz/yz})^4(d_{xy})^1(d_{z2})^0(d_{x2-y2})^0$ electronic configuration.

As shown in Figure 3c, the $Co^{1+}$ and $Ru^{3+}$ centers are magnetically coupled by either $(Ru4d_{x2-y2})$–O2p–$(Co3d_{x2-y2})$ or $(Ru4d_{z2})$–O2p-$(Co3d_{x2-y2})$ σ-type super exchange or $(Ru4d_{z2})$–$(Co3d_{z2})$ direct exchange. Given that the Ru $4d_{x2-y2}$ and $4d_{z2}$ orbitals are empty and the corresponding Co3d orbitals are half filled, all of these interactions will be ferromagnetic,[23] consistent with the low-temperature magnetization data.

The disproportionation of $Co^{2+}$ evident in $LaSrCoRuO_5$ is surprising. As noted above, other transition metal cations with $d^7$ electron counts (e.g., $Pd^{3+}$, $Pt^{3+}$, $Rh^{2+}$) are observed to disproportionate in oxide environments, driven by the presence of 'preferred' coordination sites. However, to date, this behavior has been restricted to 4d and 5d transition metals where the stronger ligand fields (compared to 3d metals) provide a larger energetic stabilization for the $d^6$ octahedral and $d^8$ square-planar electron-count/coordination combinations. It is therefore unexpected to see $Co^{2+}$, a common oxidation state with a modest ligand field in oxides, undergo a coordination-site driven disproportionation.

There are limited examples of 3d transition metal cations, such as $Fe^{4+}$ and $Ni^{3+}$ disproportionating in extended oxides. However, in these cases the disproportionation of the metal center (e.g. $Fe^{4+}$ in $CaFeO_3$ or $BaFeO_3$; $Ni^{3+}$ in $TlNiO_3$)[24–26] is driven by a metal-insulator phase transition driven by the presence of a single electron in the σ-band of these oxides phases, rather than coordination site preference.

The unique observation of coordination-site driven disproportionation of $Co^{2+}$ in $LaSrCoRuO_5$ suggests that the topochemical reaction which forms $LaSrCoRuO_5$ may act to 'select' this phase, as the disproportionated structure is a local energy minimum in composition-structure space in the reaction path between $LaSrCoRuO_6$ and $LaSrCoRuO_4$. Indeed, the same argument can be applied to the topochemical reactions which form the $Rh^{I}/Rh^{III}$ disproportionated phases reported previously.[6–7] In combination these observations suggest further coordination-site driven disproportionated oxide phases could be accessible by this type of low-temperature reaction, presenting an opportunity to prepare a range of transition metal oxides with a rich variety of novel metal oxidation-state/coordination geometry-combinations.

## Acknowledgements

Experiments at the Diamond Light Source were performed as part of the Block Allocation Group award "Oxford Solid State Chemistry BAG to probe composition-structure–property relationships in solids" (CY25166). Experiments at the ISIS pulsed neutron facility were supported by a beam time allocation from the STFC (doi.org/10.5286/ISIS.E.RB2220199). ZL and MAH thank the EPSRC (EP/T027991/1) for funding. We thank Daphne Vandemeulebroucke for assistance collecting the EELS data.

## Conflict of Interest

The authors declare no conflict of interest.

## Data Availability Statement

The data that support the findings of this study are available from the corresponding author upon reasonable request.

**Keywords:** Disproportionation · Double Perovskite Oxides · Ferromagnetism · Topochemical Reduction · Transition-Metal Oxides

[1] J. Bouvaist, D. Weigel, *Acta Crystallogr. Sect. A* **1970**, *26*, 501–510.
[2] N. Kumada, N. Kinomura, P. M. Woodward, A. W. Sleight, *J. Solid State Chem.* **1995**, *116*, 281–285.
[3] J. A. McMillan, *J. Inorg. Nucl. Chem.* **1960**, *13*, 28–31.
[4] R. V. Panin, N. R. Khasanova, C. Bougerol, W. Schnelle, G. Van Tendeloo, E. V. Antipov, *Inorg. Chem.* **2010**, *49*, 1295–1297.
[5] C. T. Prewitt, K. B. Schwartz, R. D. Shannon, *Acta Crystallogr. Sect. C* **1983**, *39*, 519–521.
[6] Z. Xu, R. G. Palgrave, M. A. Hayward, *Inorg. Chem.* **2020**, *59*, 13767–13773.
[7] Z. Y. Xu, P. K. Thakur, T. L. Lee, A. Regoutz, E. Suard, I. Puente-Orench, M. A. Hayward, *Inorg. Chem.* **2022**, *61*, 15686–15692.
[8] M. Gateshki, J. M. Igartua, *Mater. Res. Bull.* **2003**, *38*, 1893–1900.
[9] Z. Liang, M. Amano Patino, M. Hendrickx, J. Hadermann, M. A. Hayward, *ACS Org. Inorg. Au* **2022**, *2*, 75–82.
[10] M. Amano Patino, D. Zeng, R. Bower, J. E. McGrady, M. A. Hayward, *Inorg. Chem.* **2016**, *55*, 9012–9016.
[11] S. H. Kim, P. D. Battle, *J. Solid State Chem.* **1995**, *114*, 174–183.
[12] J. W. G. Bos, J. P. Attfield, *Chem. Mater.* **2004**, *16*, 1822–1827.
[13] S. Plana-Ruiz, Y. Krysiak, J. Portillo, E. Alig, S. Estrade, F. Peiro, U. Kolb, *Ultramicroscopy* **2020**, *211*.
[14] L. Palatinus, P. Brazda, M. Jelinek, J. Hrda, G. Steciuk, M. Klementova, *Acta Crystallogr. Sect. B* **2019**, *75*, 512–522.
[15] S. Aasland, H. Fjellvag, B. C. Hauback, *J. Solid State Chem.* **1998**, *135*, 103–110.
[16] A. A. Coelho, *J. Appl. Crystallogr.* **2018**, *51*, 210–218.
[17] F. Denis Romero, L. Coyle, M. A. Hayward, *J. Am. Chem. Soc.* **2012**, *134*, 15946–15952.
[18] C. F. Smura, D. R. Parker, M. Zbiri, M. R. Johnson, Z. A. Gal, S. J. Clarke, *J. Am. Chem. Soc.* **2011**, *133*, 2691–2705.

[19] N. E. Brese, M. O'Keeffee, *Acta Crystallogr. Sect. B* **1991**, *47*, 192–197.
[20] O. H. Hansteen, H. Fjellvag, B. C. Hauback, *J. Solid State Chem.* **1998**, *141*, 411–417.
[21] J. A. Alonso, M. J. MartinezLope, J. L. GarciaMunoz, M. T. FernandezDiaz, *J. Phys. Condens. Matter* **1997**, *9*, 6417–6426.
[22] O. A. Makgae, T. N. Phaahlamohlaka, B. Z. Yao, M. E. Schuster, T. J. A. Slater, P. P. Edwards, N. J. Coville, E. Liberti, A. I. Kirkland, *J. Phys. Chem. C* **2022**, *126*, 6325–6333.
[23] J. B. Goodenough, *Magnetism and the chemical bond*, Wiley, New York **1963**.
[24] M. Takano, N. Nakanishi, Y. Takeda, S. Naka, T. Takada, *Mater. Res. Bull.* **1977**, *12*, 923–928.
[25] Z. H. Tan, F. D. Romero, T. Saito, M. Goto, M. A. Patino, A. Koedtruad, Y. Kosugi, W. T. Chen, Y. C. Chuang, H. S. Sheu, J. P. Attfield, Y. Shimakawa, *Phys. Rev. B* **2020**, *102*, 054404.
[26] S. J. Kim, M. J. Martinez-Lope, M. T. Fernandez-Diaz, J. A. Alonso, I. Presniakov, G. Demazeau, *Chem. Mater.* **2002**, *14*, 4926–4932.

Manuscript received: September 5, 2023
Accepted manuscript online: December 12, 2023
Version of record online: December 12, 2023